Evaluation of Parameters Influencing S Values in Mouse Dosimetry

Cecilia Hindorf, PhD; Michael Ljungberg, PhD; and Sven-Erik Strand, PhD

Department of Medical Radiation Physics, The Jubileum Institute, Lund University, Sweden

Clinical radionuclide therapy studies are commonly preceded by studies with small animals. Reliable evaluation of therapeutic efficacy must be based on accurate dosimetry. This study was performed to evaluate the influence of the mass of organs, the shape of organs, and the distances between organs on S values for mice. **Methods:** A voxel-based version of a geometric model of a mouse was developed for input in our Monte Carlo program based on EGS4. Simulations were made for each source organ separately to resolve the S values for each organ. For verification purposes, S values were calculated for spheres of different masses and compared with the S values in the MIRDOSE3.1 software and with the S values on the Radiation Dose Assessment Resource Web site. The variation in the mass of the organs was determined from dissected mice. The influence of the shape of an organ was investigated by successive elongation of a sphere into spheroids with a constant mass. The right kidney was moved in the phantom of the mouse to evaluate the effect of organ distances on S values. The absorbed fractions for the mouse model presented here were compared with the results from some previously published models. The radionuclides used were ^{90}Y, ^{131}I, ^{111}In, and ^{99m}Tc. **Results:** The results showed that the organ mass for one animal can differ by up to 33% from the mean mass. If linear interpolation from S value tables is used to obtain an S value for the specific mass of an organ, then the S value can differ by up to 80% from its true value. The corresponding deviation obtained by scaling according to mass is 20%. The shape of an organ was found to be the least important parameter for the S value. The cross-absorbed S value is strongly dependent on the geometry and the emitted radiation. For example, a 9.2-mm movement of the kidney can cause the S value from the liver to the right kidney to decrease to 0.05% of its original value for ^{90}Y. **Conclusion:** We conclude that the mass and the shape of organs and their locations relative to each other have considerable effects on mouse dosimetry.

Key Words: dosimetry; mouse; S values; radionuclide therapy

J Nucl Med 2004; 45:1960–1965

Small-animal dosimetry is important in the evaluation of new radiopharmaceuticals for radionuclide therapy, because preclinical studies are usually performed with animals before new radiopharmaceuticals are introduced into clinical applications. The absorbed dose is the quantity that should be used, because it is generally believed to be related to the biologic effect via absorbed dose–response relationships, as has been shown for external radiation therapy. For appropriate preclinical absorbed dose–response or absorbed dose–effect relationships to be obtained, the absorbed dose must be determined as exactly as possible. An accurate anatomic description of the relevant species is therefore essential, because the cross-absorbed dose between different organs and tissues can be significant (the cross-absorbed dose has been reported to constitute up to 70%–75% of the total absorbed dose in mice when ^{90}Y is used (*1*)) and is strongly dependent on a correct description of the anatomy. If the geometry is incorrect, then the cross-absorbed doses between organs will not be accurately calculated, leading to inaccuracy in the total absorbed dose.

The most common method of calculating the absorbed dose to a target region from radiation emitted from a source region is by the MIRD formulation, defined by the MIRD Committee (*2*). The mean absorbed dose in this formulation is the product of the cumulated activity (defined as the total number of disintegrations during the relevant time interval) and an appropriate S value (the absorbed dose to the target region per radioactive disintegration in the source region). The S value is defined as the product of the emitted energy per disintegration and the absorbed fraction for the given combination of source and target regions and for the type of radiation emitted divided by the mass of the target region. S values therefore are strongly dependent on the geometry of both the source region and the target region and on the quality of the emitted radiation. S values are generally calculated for anatomic models with the Monte Carlo method or dose kernels for both animals and humans.

Some anatomic models of mice have been published. The models presented by Hui et al. (*3*) and Flynn et al. (*4*) rely on a simplified geometry in which the organs are modeled as combinations of ellipsoids, spheroids, and cylinders. The organs are derived from mean values of organ mass, organ shape, and position of the organs in a cohort of animals. In

Received Apr. 6, 2004; revision accepted May 20, 2004.

For correspondence or reprints contact: Cecilia Hindorf, PhD, Department of Medical Radiation Physics, The Jubileum Institute, Lund University Hospital, SE-221 85 Lund, Sweden.

E-mail: Cecilia.Hindorf@radfys.lu.se

a recent publication, Kolbert et al. (*5*) described a phantom in which the organs of a single mouse were segmented from high-resolution MR images, giving a voxel-based phantom. The advantage of this approach is that the anatomy is more geometrically realistic than is that in the analytically described models. The drawbacks are that this type of phantom represents one unique animal and that it is difficult to modify the relative shapes, sizes, and locations of organs.

It is of importance to evaluate the dependence of the absorbed fraction on different parameters and S values when one is considering the accuracy of preclinical dosimetry. The aim of this study was therefore to investigate some of these parameters and their relationships with a geometric model of a mouse. The parameters studied for various radionuclides were the organ mass, the organ shape, and the distance between neighboring organs.

MATERIALS AND METHODS

A mathematic model of a mouse, based on anatomic data from animals dissected at our laboratory and images in anatomic atlases of mice (*6*), was developed by combination of simple geometric shapes, the equations for which are given in the Appendix. The masses of included organs are shown in Table 1, and an illustration of the mouse model is shown in Figure 1. This model is comparable to previously described common mathematic phantoms for humans (*7*). From the analytic description of the mathematic model, a voxel-based image version of the mouse model was generated by use of a program written in IDL (Research System Inc.). The matrix dimensions were 64 × 64 × 166, with a cubic voxel size equal to 0.39 mm. The images were used as input to an EGS4 Monte Carlo program, from which 3-dimensional images of the energy deposition, with the same dimensions as the input images, were calculated. Each of the organs was simulated separately, and the absorbed fractions and related S values were calculated from the individual energy deposition images.

To verify the accuracy of the method of generating voxel-based models of an analytic shape, we performed Monte Carlo simulations of spheres of different sizes uniformly filled with different radionuclides and calculated the S values. The self-absorbed S values for unit-density spheres of masses that varied between 1 and 300 g were calculated and compared with the S values given by the nodule module in the MIRDOSE3.1 software (*8*) and the S values on the Radiation Dose Assessment Resource (RADAR) Web site (*9*). All Monte Carlo simulations were performed for 4 radionuclides (^{99m}Tc, ^{90}Y, ^{131}I, and ^{111}In). The simulations were performed by use of a computer with a 2,400-MHz AMD processor running Linux Redhat 8.0. The EGS4 program was compiled with a Lahey/Fujitsi Fortran-95 version 6.2 compiler. A typical run time (1 source organ) for ^{99m}Tc and ^{111}In was 1.5 h, and for ^{90}Y, the calculation time was about 6 h. The number of histories for each source region and radionuclide was 30 million. The accuracy of the simulations was within 2% that for the self-absorbed fractions and within 5% that for the cross-absorbed fractions for ^{111}In, ^{131}I, and ^{99m}Tc. For ^{90}Y, the accuracy of the cross-absorbed fractions was highly dependent on the distance and varied from less than 1% to 18%. Bremsstrahlung was included in the Monte Carlo simulations.

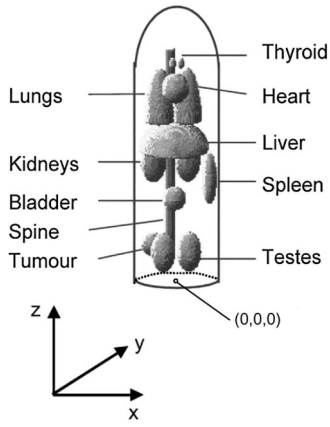

FIGURE 1. Anatomic model of a mouse presented in this work.

TABLE 1
Masses of Organs Included in Anatomic Model of Mouse

Organ or sample	Mass (g)
Total body	24
Bladder	0.03
Heart	0.12
Kidneys	0.28
Liver	0.89
Lungs	0.15
Spine	0.19
Spleen	0.09
Testes	0.25
Thyroid	0.02
Tumor	Optional
Urine	0.03

Evaluations regarding changes in organ mass, shape, and distance between the organs were performed for each of the 4 radionuclides. The activity distribution within all the organs was defined in the program to be uniform. The density distribution for each organ was also defined to be uniform and was set to 1 g/cm^3, except for the lungs and the spine, for which 0.3 and 1.4 g/cm^3 were used, respectively. The cutoff energy (i.e., the limit at which the energy is regarded to be locally absorbed) was set to 10 keV for the photons and 40 keV for the electrons in all simulations. The range of a 40-keV electron (29 μm in water) was regarded as sufficiently small compared with the size of a voxel (0.39 mm).

Organ Mass

To evaluate the variations in organ mass from animal to animal, the mean, the minimum, and the maximum masses of the total body, the liver, and the right kidney were determined from 10 dissected mice of the same breed, sex, and age.

The variations in the S values for an organ attributable to its variations in mass were determined by generating corresponding uniform spheres with masses equal to the mean, the minimum, and the maximum masses of the 3 "organs" (total body, liver, and right kidney). The S values were Monte Carlo simulated by the method described above and also were calculated from data obtained from the RADAR Web site either by linear interpolation or by scaling according to organ mass.

Interpolation was performed by weighting the 2 nearest S values obtained from the RADAR database to give the S value for the actual mass of the organ ($S_{Interpol}$) as follows:

$$S_{Interpol} = S_{Sph1} + \left[\frac{S_{Sph2} - S_{Sph1}}{m_{Sph2} - m_{Sph1}} \cdot (m_{Organ} - m_{Sph1})\right], \quad \text{Eq. 1}$$

where S_{Sph1} is the S value for sphere 1, that with the nearest lower mass relative to that of the organ; S_{Sph2} is the S value for sphere 2, that with the nearest higher mass relative to that of the organ; m_{Sph1} is the mass of sphere 1; m_{Sph2} is the mass of sphere 2; and m_{Organ} is the mass of the organ being modeled.

Scaling was performed to obtain the S value for the organ (S_{Scaled}) as follows:

$$S_{Scaled} = S_{Sph} \cdot \frac{m_{Sph}}{m_{Organ}}, \quad \text{Eq. 2}$$

where S_{Sph} is the S value for the sphere nearest in mass, taken from tables at the RADAR Web site, m_{Sph} is the mass of the sphere, and m_{Organ} is the mass of the organ of the mouse.

Organ Shape

The importance of modeling the exact shape of an organ was investigated by successive elongation of spheroids with constant masses. The masses of the spheroids were 0.1, 1, and 10 g, and the ratios of the long axis to the short axis of the spheroids were 1, 2, 5, and 10.

Organ Separation

To evaluate the effect of the distance between organs on the S values, the right kidney was moved down 2.3, 4.6, 6.9, and 9.2 mm (corresponding to 25%, 50%, 75%, and 100% of the total kidney height, respectively). The S values from the right kidney to the left kidney ($S_{\text{Left Kidney}\leftarrow\text{Right Kidney}}$) and from the right kidney to the liver ($S_{\text{Liver}\leftarrow\text{Right Kidney}}$) then were calculated.

RESULTS

The ratios of the S values generated by the methods described in this work and data from MIRDOSE3.1 and RADAR are shown in Figures 2A and 2B, respectively. As shown in Figure 2A, the discrepancy in most data points was less than ±5% and at most 13% for ^{111}In. The best results were obtained for ^{90}Y. Compared with the RADAR data, our results showed an undercorrection for the ^{90}Y data of up to 10% for the smallest sphere.

The average and the range for the total body mass for the 10 mice were found to be 26.4 g and 21.8–31.1 g, respectively. The average masses of the liver and the right kidney were found to be 1.55 g (range, 1.11–1.83 g) and 0.21 g (range, 0.14–0.27 g), respectively. These results show that the organ mass for an individual animal can differ by up to 33% from the mean mass.

The Monte Carlo–simulated S values and the interpolated and scaled values for spheres with masses equal to the minimum, the mean, and the maximum masses of the total body, the liver, and the right kidney of the mice are shown in Table 2. For ^{90}Y and ^{131}I, the S values interpolated from the RADAR data differed by up to 80% from the Monte Carlo–simulated values. When scaled according to mass, the S values differed from the Monte Carlo–simulated values by up to 20%, the higher deviations being observed for ^{111}In and ^{99m}Tc. The highest deviation was seen for the smallest spheres.

The absorbed fractions for elongated spheroids are shown in Figure 3, in which data are shown for spheroids with masses of 10, 1, and 0.1 g. These data show that the magnitude of the absorbed fraction and thus the S values decreased gradually when the shape was changed from a sphere to an elongated spheroid. The difference was largest for ^{90}Y and for the 0.1-g spheroid, because this radionuclide emits electrons with high kinetic energy and the absorption of the energy therefore is highly geometry dependent.

Figure 4 shows the variations in $S_{\text{Left Kidney}\leftarrow\text{Right Kidney}}$ and $S_{\text{Liver}\leftarrow\text{Right Kidney}}$ when the right kidney was moved down. The variations were most pronounced for ^{90}Y, for which $S_{\text{Liver}\leftarrow\text{Right Kidney}}$ decreased to 0.05% of its initial value. For the other radionuclides (^{99m}Tc, ^{111}In, and ^{131}I), which emit both photons and electrons, the relative S value decreased to approximately 30%.

When the self-absorbed fractions for ^{90}Y obtained from the mouse models presented by Hui et al. (*3*), Flynn et al. (*4*), and Kolbert et al. (*5*) were compared with those obtained from the mouse model described in this work, we found no significant differences. The results of these comparisons are shown in Table 3. There was generally good agreement between the different models. The largest difference was found for the lungs, for which our model predicted a self-absorbed fraction of 0.22 and the other models predicted values of 0.29 and 0.31.

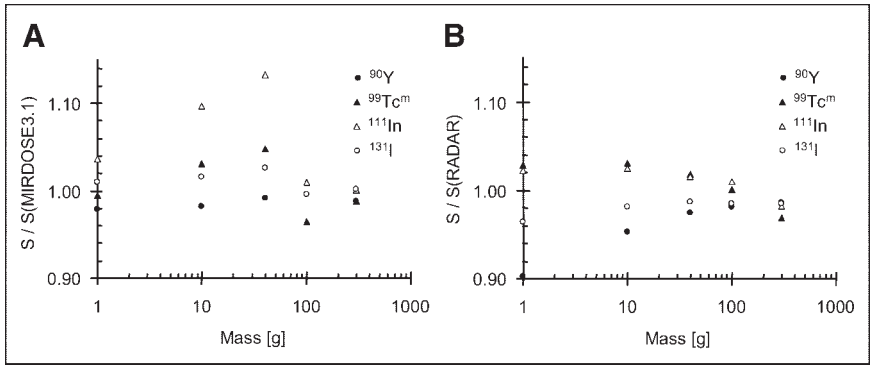

FIGURE 2. Ratios of S values obtained in this work and those obtained from other sources for spheres between 1 and 300 g for ^{90}Y, ^{99m}Tc, ^{111}In, and ^{131}I. (A) Values from MIRDOSE3.1. (B) Values from RADAR Web site.

TABLE 2
Effects of Variations in Organ Masses on Self-Absorbed S Values for 4 Radionuclides

Organ	Mass (g)*	S value (mGy/MBq/s) calculated by indicated method† for:											
		^{90}Y			^{99m}Tc			^{111}In			^{131}I		
		MC	Scaled	Interpol	MC	Scaled	Interpol	MC	Scaled	Interpol	MC	Scaled	Interpol
Right kidney	0.14	5.07E-1	5.60E-1	7.27E-1	1.85E-2	1.68E-2	2.16E-2	4.17E-2	3.51E-2	4.53E-2	2.00E-1	2.07E-1	2.67E-1
	0.21	3.70E-1	3.73E-1	6.26E-1	1.24E-2	1.12E-2	1.83E-2	2.81E-2	2.34E-2	3.84E-2	1.34E-1	1.38E-1	2.27E-1
	0.26	3.15E-1	3.02E-1	5.55E-1	1.02E-2	9.04E-3	1.60E-2	2.31E-2	1.89E-2	3.35E-2	1.10E-1	1.12E-1	1.98E-1
Liver	1.11	9.40E-2	1.03E-1	1.08E-1	2.07E-3	2.42E-3	2.55E-3	5.91E-3	5.76E-3	6.06E-3	2.69E-2	2.78E-2	2.92E-2
	1.55	7.02E-2	7.82E-2	8.46E-2	1.82E-3	1.78E-3	1.97E-3	4.36E-3	4.34E-3	4.72E-3	1.95E-2	2.01E-2	2.25E-2
	1.83	6.04E-2	6.62E-2	6.97E-2	1.55E-3	1.51E-3	1.60E-3	3.75E-3	3.67E-3	3.88E-3	1.65E-2	1.70E-2	1.82E-2
Total body	21.8	6.05E-3	6.24E-3	6.50E-3	1.53E-4	1.48E-4	1.54E-4	4.03E-4	3.91E-4	4.09E-4	1.49E-3	1.51E-3	1.58E-3
	26.4	5.03E-3	5.15E-3	5.73E-3	1.28E-4	1.22E-4	1.37E-4	3.41E-4	3.23E-4	3.65E-4	1.24E-3	1.25E-3	1.39E-3
	31.1	4.29E-3	4.45E-3	4.95E-3	1.10E-4	1.10E-4	1.19E-4	2.96E-4	3.01E-4	3.19E-4	1.06E-3	1.08E-3	1.20E-3

*Masses are listed as minimum, mean, and maximum, from top to bottom, for each organ.
†Methods were Monte Carlo (MC), scaling according to mass (Scaled), and linear interpolation (Interpol).

DISCUSSION

In this work, we used the Monte Carlo method to evaluate parameters in models used for mouse dosimetry. We developed a model for the mouse and compared our results with published data. Because there are discrepancies between a simple mathematic model of a mouse and its real anatomy, the relevance of the use of such models for internal dosimetry for mice was evaluated. A mathematic model represents mean values for organ mass, shape, and position, whereas a segmentation model represents only an individual animal.

The masses of organs may differ significantly between different individuals, as shown in this work. Scaling by mass from published S values is a better method than linear interpolation, because S values are inversely proportional to mass, even though the scaled S value is based on only one S value and thus on only one absorbed fraction, whereas the S value calculated from linear interpolation is based on two S values and absorbed fractions. For the radionuclides investigated, linear interpolation for small spheres resulted in errors in S values of up to 80%.

The shape of an organ proved to be a less important factor for self-absorbed S values than the mass of an organ. For example, when the ratio of the long axis to the short axis of the spheroid was 2, the change in the S values for the radionuclides investigated was at most 5% of the S values for a sphere.

We found that the distance between the organs strongly influenced the cross-absorbed S values, especially for ^{90}Y. This radionuclide emits only β-particles with a high maximum electron energy (2.28 MeV). For the other radionuclides investigated in this work (^{99m}Tc, ^{111}In, and ^{131}I), the distance between the organs was large in relation to the maximum electron range. It was therefore mainly the energy deposition resulting from photons that caused the change in

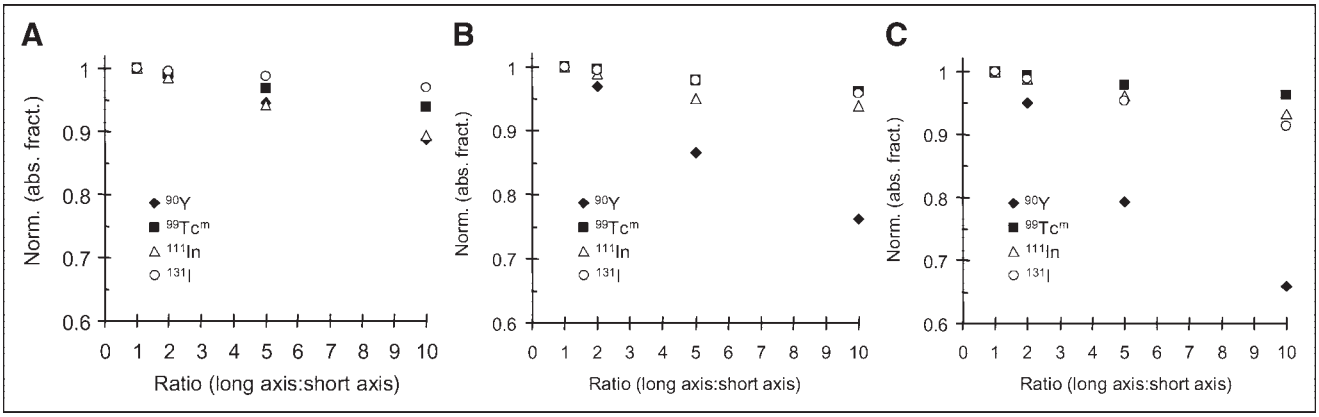

FIGURE 3. Relative absorbed fractions (abs. fract.) for spheroids with a constant mass and various ratios of the long axis to the short axis. (A) Mass, 10 g. (B) Mass, 1 g. (C) Mass, 0.1 g. Norm. = normalized.

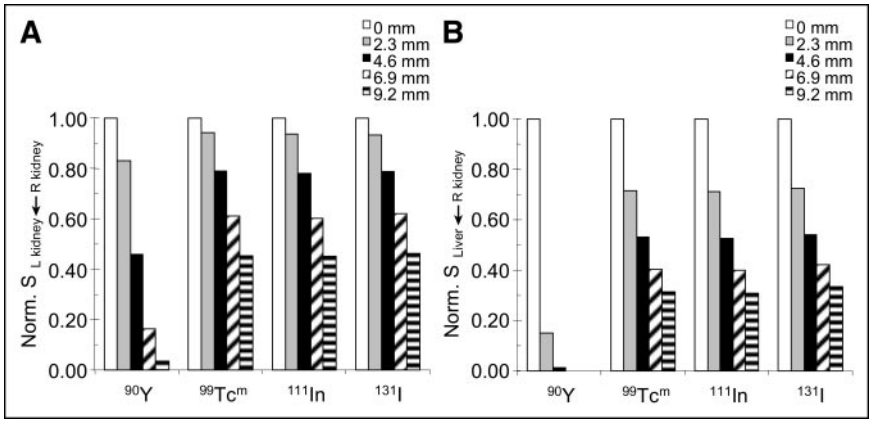

FIGURE 4. Cross-absorbed S values normalized (Norm.) to those at the original position of the kidney and the kidney moved down 2.3, 4.6, 6.9, and 9.2 mm. (A) $S_{\text{Left Kidney}\leftarrow\text{Right Kidney}}$. (B) $S_{\text{Liver}\leftarrow\text{Right Kidney}}$.

the S values when the distance between organs was altered. The similarities seen in Figure 4 for the normalized cross-absorbed S values for the three photon-emitting radionuclides were attributable to the relatively small variations in the mean-free path-length in water for the photon energies in question (6.5 cm for 140 keV and 9.1 cm for 364 keV).

The differences in the results between the models (Table 3) can be explained by the fact that the absorbed fractions were calculated with different calculation procedures. We used full Monte Carlo simulations for both electrons and photons; density differences as well as body boundaries were considered in these simulations. The approach of Kolbert et al. (*5*) involved the use of a convolution procedure with dose kernels obtained in a uniform medium.

An interesting finding is that the model presented by Kolbert et al. (*5*), which should provide the most accurate geometric form for the animal organs, produces results fairly similar to those produced by more general geometric approaches. It is difficult to estimate the distances between individual organs from mathematic models and, as a result, the cross-absorbed S values are probably less accurate in these models than in those based on image segmentation. Because of the small dimensions of a mouse, the cross-absorbed doses between organs depend greatly on the energy of the emitted electrons. In principle, a more accurate description of the anatomy is required, and the work by Kolbert et al. and the voxel-based segmented phantoms may be an important step in this direction.

TABLE 3
Comparisons of Self-Absorbed Fractions for ^{90}Y in Different Dosimetric Models of Mice

	Self-absorbed fraction reported by:			
Organ	Hui et al. (*3*)	Flynn et al. (*4*)	Kolbert et al. (*5*)	Us (this work)
Heart	0.45	0.49	N/A	0.47
Kidneys	0.46	N/A*	0.54 and 0.51†	0.48
Liver	0.67	0.69	0.69	0.64
Lungs	0.29	0.31	N/A	0.22
Spleen	0.34	0.37	0.34	0.38
Total body	0.88	N/A	N/A	0.86

*Flynn et al. presented detailed model of kidneys that did not give absorbed fractions comparable to others.

†Kolbert et al. presented absorbed fractions for two kidneys separately.

N/A = not available.

CONCLUSION

We conclude that the mass and the shape of organs and their locations relative to each other have considerable effects on mouse dosimetry, that the mass is the most important parameter for self-absorbed S values, and that the distance between the organs is the most important parameter for cross-absorbed S values.

The fact that anatomic variations between individuals can be considerable places a limit on the accuracy of dosimetry based on simple mathematic representations of the anatomy (mean value representation) as well as on that of models based on organ segmentation from anatomic images (single-animal representation).

APPENDIX

The equations representing the mouse model presented in this work are as follows. Equations 1A, 2A, 4A, 6A, and 7A are valid within the given limits of z.

For the trunk,

$$\left(\frac{x}{1.1}\right)^2+\left(\frac{y}{1.2}\right)^2\le 1,\qquad 0.0\le z\le 4.7. \quad \text{Eq. 1A}$$

For the head,

$$\left(\frac{x}{1.1}\right)^2+\left(\frac{y}{1.2}\right)^2+\left(\frac{z-4.7}{1.6}\right)^2\le 1,\qquad z>4.7. \quad \text{Eq. 2A}$$

For the heart,

$$\left(\frac{x}{0.29}\right)^2+\left(\frac{y+0.55}{0.32}\right)^2+\left(\frac{z-4.2}{0.32}\right)^2\le 1. \quad \text{Eq. 3A}$$

For the spine,

$$\left(\frac{x}{0.1}\right)^2 + \left(\frac{y-1}{0.1}\right)^2 \le 1, \qquad z \le 4.7. \quad \text{Eq. 4A}$$

For the kidneys,

$$\left(\frac{x \pm 0.4}{0.27}\right)^2 + \left(\frac{y-0.7}{0.27}\right)^2 + \left(\frac{z-2.2}{0.46}\right)^2 \le 1. \quad \text{Eq. 5A}$$

For the liver,

$$\left(\frac{x+0.2}{0.8}\right)^2 + \left(\frac{y+0.15}{0.85}\right)^2 + \left(\frac{z-2.7}{0.6}\right)^2 \le 1, \qquad z \ge 2.7.$$

Eq. 6A

For the lungs,

$$\left(\frac{x \pm 0.32}{0.32}\right)^2 + \left(\frac{y}{0.32}\right)^2 + \left(\frac{z-3.3}{1.2}\right)^2 \le 1, \qquad z \ge 3.3.$$

Eq. 7A

For the spleen,

$$\left(\frac{x-0.8}{0.15}\right)^2 + \left(\frac{y+0.5}{0.25}\right)^2 + \left(\frac{z-2.1}{0.57}\right)^2 \le 1. \quad \text{Eq. 8A}$$

For the testes,

$$\left(\frac{x \pm 0.3}{0.26}\right)^2 + \left(\frac{y+0.8}{0.26}\right)^2 + \left(\frac{z-0.5}{0.44}\right)^2 \le 1. \quad \text{Eq. 9A}$$

For the thyroid,

$$\left(\frac{x \pm 0.1}{0.05}\right)^2 + \left(\frac{y+1}{0.05}\right)^2 + \left(\frac{z-4.9}{0.11}\right)^2 \le 1. \quad \text{Eq. 10A}$$

For the bladder,

$$\left(\frac{x}{0.25}\right)^2 + \left(\frac{y+0.3}{0.25}\right)^2 + \left(\frac{z-1.6}{0.25}\right)^2 \le 1. \quad \text{Eq. 11A}$$

ACKNOWLEDGMENTS

The authors acknowledge Magnus Tagesson, Melinda Joó, and Liu Xiaowei for important contributions to this work. This work was supported by grants from the Swedish Cancer Society; the Berta Kamprad Foundation; and the Gunnar, Arvid, and Elisabeth Nilsson Foundation.

REFERENCES

1. Beatty BG, Kuhn JA, Hui TE, Fisher DR, Williams LE, Beatty JD. Application of the cross-organ beta dose method for tissue dosimetry in tumor-bearing mice treated with a 90-Y-labeled immunoconjugate. *Cancer*. 1994;73:958–965.
2. Loevinger R, Budinger TF, Watson EE. *MIRD Primer for Absorbed Dose Calculations*. New York, NY: The Society of Nuclear Medicine; 1991.
3. Hui TE, Fisher DR, Kuhn JA, et al. A mouse model for calculating cross-organ beta doses from yttrium-90-labeled immunoconjugates. *Cancer*. 1994;73:951–957.
4. Flynn AA, Green AJ, Pedley RB, et al. A mouse model for calculating the absorbed beta-particle dose from ^{131}I- and ^{90}Y-labeled immunoconjugates, including a method for dealing with heterogeneity in kidney and tumor. *Radiat Res*. 2001;156:28–35.
5. Kolbert KS, Watson T, Matei C, Xu S, Koutcher JA, Sgouros G. Murine S factors for liver, spleen, and kidney. *J Nucl Med*. 2003;44:784–791.
6. Cook MJ. *The Anatomy of the Laboratory Mouse*. London, U.K.: Academic Press; 1965.
7. International Commission on Radiation Units and Measurements, Inc. ICRU report 48: phantoms and computational models in therapy, diagnosis and protection. Oxford, U.K.: Oxford University Press; 1992.
8. Stabin MG. MIRDOSE: personal computer software for internal dose assessment in nuclear medicine. *J Nucl Med*. 1996;37:538–546.
9. Stabin MG, Siegel JA. Physical models and dose factors for use in internal dose assessment. *Health Phys*. 2003;85:294–310.